Research Square

Preprints are preliminary reports that have not undergone peer review.
They should not be considered conclusive, used to inform clinical practice,
or referenced by the media as validated information.

Arsenic Drives Mitophagic Cell Death via mtROS-Nrf2-PINK1/Parkin Axis in Prostate Stromal Cells

Yiping Yang
Guangxi Medical University Cancer Hospital
Yi Huang
Guangxi Medical University Cancer Hospital
Yangchao Jiang
Guangxi Medical University Cancer Hospital
Chunlin Zhang
Guangxi Medical University Cancer Hospital
Wenqiang Lu
Guangxi Medical University Cancer Hospital
Guanglin Yang
Guangxi Medical University Cancer Hospital
Qingyun Zhang
Guangxi Medical University Cancer Hospital
Yingxi Mo
Guangxi Medical University Cancer Hospital
Shan Wang
wangshan@sr.gxmu.edu.cn

Guangxi Medical University Cancer Hospital

Research Article

Keywords: Arsenic, mtROS, Nrf2, Mitophagy, Prostate damage

Posted Date: November 23rd, 2026

DOI: https://doi.org/10.21203/rs.3.rs-11151757/v1

License: This work is licensed under a Creative Commons Attribution 4.0 International License.
Read Full License

Additional Declarations: No competing interests reported.

Abstract

Chronic exposure to inorganic arsenic through contaminated drinking water and food is a recognized risk factor for prostate diseases; however, the mechanism by which arsenic disrupts prostate stromal homeostasis remains poorly defined. Here, we revealed that sodium arsenite induced mitochondrial damage in human prostate stromal WPMY-1 cells and triggered PINK1/Parkin-dependent mitophagy. Arsenic exposure rapidly elevated mitochondrial reactive oxygen species (mtROS), which stimulated Nrf2 nuclear translocation. Unexpectedly, this Nrf2 activation was essential for mitophagy induction rather than canonical antioxidant defense, and pharmacological blockade of Nrf2 completely abolished PINK1/Parkin upregulation and autophagosomal engulfment of mitochondria. In mice, chronic arsenic ingestion caused prostatic hyperplasia accompanied by elevated Nrf2, PINK1, Parkin, and LC3-II levels. Our data establish an arsenic-mtROS-Nrf2-PINK1/Parkin mitophagy signaling cascade that disrupts mitochondrial quality control in the prostate stroma, revealing a noncanonical pro-mitophagic function of Nrf2. Targeting this axis may provide a therapeutic avenue for arsenic-associated prostatic pathologies.

Introduction

Arsenic, a ubiquitous environmental toxicant, continues to pose substantial public health challenges due to its pervasive presence in drinking water, soil, and food sources worldwide. Inorganic arsenic primarily exists in two oxidation states, arsenite (As^{3+}) and arsenate (As^{5+}), which undergo biotransformation in the body through methylation, producing monomethylarsonic acid (MMA) and dimethylarsinic acid (DMA) (El-Ghiaty and El-Kadi, 2023). Chronic exposure to arsenic has been implicated in a wide spectrum of pathologies, ranging from carcinogenesis to metabolic and reproductive disorders (Peng et al. 2022; Zhang et al. 2025; Zhang et al. 2026). The prostate, a critical organ in the male reproductive system, has been consistently identified as a primary target of arsenic toxicity (Xie et al. 2020; Yang et al. 2025). Our recent studies established that arsenic triggers malignant transformation and PANoptosis in prostate stromal cells by inducing mitochondrial damage (Yang et al. 2024c; Yang et al. 2025). However, whether arsenic simultaneously provokes mitophagy as a compensatory response remains unclear.

Mitophagy is a key quality control mechanism by which cells clear dysfunctional or superfluous mitochondria to maintain intracellular homeostasis. Mitophagy can proceed via canonical and noncanonical pathways (Picca et al. 2023). Noncanonical mitophagy may be induced under cellular stress, leading to dysfunctional mitochondrial renovation (Picca et al. 2023). Canonical mitophagy operates through two major routes. Receptor-mediated mitophagy involves BNIP3, NIX/BNIP3L, and FUNDC1, which directly recruit LC3-coated phagophores under hypoxic or metabolic stress (Picca et al. 2023; Wang et al. 2023). PINK1/Parkin-mediated pathway involves PINK1 accumulation, Parkin recruitment, and phosphor(p)-Ub chain generation. PINK1 serves as a damage-specific sensor. In healthy mitochondria, PINK1 is rapidly degraded; upon depolarization, PINK1 accumulates on the outer membrane, recruits and phosphorylates the E3 ligase Parkin, and generates p-Ub chains. The p-Ub chains are recognized by autophagic adapters (P62, TAX1BP1, and OPTN) and subsequently delivered to lysosomes for degradation (Picca et al. 2023; Wang et al. 2023). Emerging research has reported that

PINK1/Parkin-dependent mitophagy is implicated in arsenic-induced hepatic fibrosis and acute kidney injury (Liu et al. 2023; Wu et al. 2026); however, the regulatory effects of arsenic-induced mitophagy in prostate cells remain unknown.

Nuclear factor (erythroid-2 related) factor 2 (Nrf2) is a key transcription factor that regulates cellular defense against toxic and oxidative stress responses. Under basal conditions, Nrf2 binds to Keap1 in its Neh2 domain by DLG and ETGE motifs and leads to proteasomal degradation. Upon oxidative stress, Nrf2 dissociates from Keap1, translocates to the nucleus, and activates antioxidant gene expression (Kobayashi et al. 2004; Kobayashi et al. 2006). It is well established that arsenic-damaged mitochondria lead to disrupted mitochondrial integrity, mitochondrial reactive oxygen species (mtROS) overproduction, and exacerbated oxidative stress (Yang et al. 2025; Wei et al. 2020). ROS and mtROS formation are reciprocally regulated by Nrf2 (Bjorkman and Pereira, 2021; Cantoni et al. 2022; Jiang et al. 2024). Besides, studies revealed that arsenic exposure modulates Nrf2 expression; however, its effect, whether promoting or inhibiting, varies across different tissue and cell types (Xie et al. 2020; Yang et al. 2024b). Consequently, it is crucial to elucidate whether arsenic exposure-triggered ROS and mtROS are vital for activating Nrf2 during arsenic-induced prostate damage.

Besides antioxidant responses, Nrf2 signaling modulates mitochondrial homeostasis and mitophagy (O'Mealey et al. 2017; Song et al. 2023). Emerging studies have demonstrated that Nrf2 regulates both the transcriptional expression of mitochondrial quality control under stress conditions by modulating key mitophagic regulators, including PINK1 (Li et al. 2026; Murata et al. 2015; Xiao et al. 2017). Furthermore, Nrf2 activation promotes PINK1/Parkin-dependent mitophagy in hepatic and brain injury (Song et al. 2023; Li et al. 2026). However, whether arsenic-induced oxidative stress activates Nrf2 to serve as a functional mediator of PINK1/Parkin-dependent mitophagy in prostate stromal cells remains elusive.

For the above reasons, *in vitro* and *in vivo* models were designed to study arsenic-induced mitophagy in the prostate, focusing on the mtROS-Nrf2- PINK1/Parkin signaling cascade. These findings aimed to advance our mechanistic understanding of arsenic-induced prostatic injury and identify potential therapeutic targets.

Materials and Methods

Cell Culture and Treatment

WPMY-1 cells (ATCC) were cultured in Dulbecco's Modified Eagle Medium (DMEM; Servicebio, Hubei, China) supplemented with 5% (v/v) fetal bovine serum (FBS; F103-01; Vazyme, Nanjing, China), 100 U mL^{-1} penicillin, and 100 μg mL^{-1} streptomycin (100×; Solarbio, Beijing, China). Cells were maintained in a humidified incubator at 37°C with 5% CO_2. Cells were cultured until they reached 50% confluence and then divided into groups treated with 0, 1, 2, and 4 μM sodium arsenite ($NaAsO_2$; S7400; Sigma-Aldrich, Missouri, USA) for 48 h.

The mitochondrial ROS scavenger Mito-TEMPO (HY-125944, MCE) was used as follows: Cells were pre-treated with 60 μM Mito-TEMPO for 6 hours, followed by exposure to 4 μM $NaAsO_2$ for 48 h.

For the ROS scavenger N-acetylcysteine (NAC, HY-B0215, MCE) treatment group, cells were simultaneously exposed to 4 μM $NaAsO_2$ and 2 mM NAC for 48 h. The autophagy inhibitor chloroquine (CQ; 12.5 μM) was used to pretreat cells for 3 h. The Nrf2 inhibitor ML385 (5 μM) was administered for 3 h.

For the mitochondrial permeability transition pore (mPTP) inhibitor cyclosporin A (CsA) treatment, cells were simultaneously exposed to 4 μM $NaAsO_2$ and 200 nM CsA (HY-B0579, MCE) for 48 h.

Mitochondrial ROS Detection

MitoSOX™ Red (MCE, HY-D1055) was prepared as a 5 mM stock solution in high-purity DMSO and stored at -20°C in the dark. After drug treatment, MitoSOX was diluted to 4 μM in FBS-free DMEM and incubated for 15 min at 37°C. Cells from different groups were gently washed twice with PBS and subsequently imaged using fluorescence microscopy (Axio Observer 3; Zeiss, Germany) with an excitation wavelength of 510 nm and an emission filter of 580 nm. For quantitative analysis, 6 random fields (≈ 20 cells/field) were selected from each dish.

Intracellular Total ROS Measurement

The oxidation-sensitive probe 2',7'-dichlorofluorescin diacetate (DCFH-DA, MCE, HY-D0940) was used to assess intracellular ROS. Following treatment, 5 μM DCFH-DA was added, and the cells were incubated in the dark at 37°C for 30 min. The cells were then gently washed twice with PBS before imaging. The excitation wavelength was 488 nm, and the emission filter was 525 nm.

Mitochondrial Membrane Potential (MMP) Assessment

The lipophilic cationic dye JC-1 (Beyotime, C2006) was used. After treatment, the cells were incubated with 2 μg/L JC-1 at 37°C for 20 min, washed twice with PBS, and then observed under an Axio Observer 3 (Zeiss, Germany). JC-1-aggregates, indicative of mitochondrial membrane polarization, were excited at 588 nm with an emission filter of 590 nm. JC-1 monomers, indicative of mitochondrial depolarization, were excited at 514 nm with an emission filter of 529 nm. The ΔΨm index was represented as the ratio of red/green integrated fluorescence density of individual cells.

Transmission Electron Microscopy (TEM)

For TEM analysis, WPMY-1 cells were divided into a control group and an arsenic-treated groups to compare ultrastructural changes. After the treatments, cells were harvested by centrifugation and fixed

in TEM fixative (Servicebio, G1102) at 4°C for 2–4 h, and post-fixed with 1% osmium tetroxide in 0.1 M phosphate buffer (pH 7.4) for 2 h. Next, the cells were dehydrated, embedded in Epon-812, and polymerized at 60°C for 48 h. Ultrathin sections were observed using an HT7800 TEM (Hitachi, Tokyo, Japan) transmission electron microscope.

Immunofluorescence

After treatment with 0 or 4 μM $NaAsO_2$ for 48 h, the cells were fixed with 1:1 acetone/methanol for 10 min, permeabilized with 0.05% Triton X-100 for 5 min, and blocked with 2% BSA at 37°C for 30 min. Subsequently, cells were incubated with antibody (LC3, Proteintech 14600-1-AP, 1: 300; Tomm20, Abcam ab56783, 1: 500; PINK1, Cloud-clone corp PAL057Mu01, 1: 300; Parkin, Zenbio R381626, 1: 200; Nrf2, Proteintech 16396-1-AP, 1: 400) for 1 h, washed three times with PBS, and then incubated in the dark with a fluorescent secondary antibody diluted 1:1000 (VF298231; Invitrogen) for 1 h. Nuclei were stained with DAPI (28718-90-3; BioFroxx) for 5 min, and images were captured using a Zeiss LSM 800 laser confocal microscope.

Reverse Transcription quantitative Polymerase Chain Reaction (RT-qPCR)

Total RNA was extracted using TRIzol, and reverse transcription was performed using PrimeScript RT Master Mix (Takara) to synthesize cDNA. RT-qPCR was then conducted on an Applied Biosystems™ 7500 Real-Time PCR System using SYBR Green (Bio-Rad). The primers used for qPCR included PINK1, Parkin, LC3, and SQSTM1. The primer sequences are listed in TableS1.

Subcellular Fractionation

The cells were harvested, washed with ice-cold PBS, and resuspended in hypotonic lysis buffer. After 15 min of incubation on ice, the cells were homogenized and centrifuged at 800 × g for 10 min at 4°C. The supernatant was collected as the cytoplasmic fraction. The pellet was resuspended in nuclear extraction buffer, incubated on ice for 30 min, and centrifuged at 14000 × g for 15 min at 4°C. The resulting supernatant was collected as the nuclear fraction. For mitochondrial isolation, the crude pellet was resuspended in mitochondrial buffer, layered onto a sucrose step gradient, and centrifuged at 15000 ×g for 20 minutes at 4°C. The mitochondrial band was collected, washed, and resuspended in radioimmunoprecipitation assay (RIPA) buffer.

Western Blotting

Post-treatment cells were lysed and quantified using the Pierce™ BCA Protein Assay Kit (Thermo Scientific). Proteins were transferred from 4% to 20% gel to a 0.22 μm BioTrace™ NT NC membrane (66485; Pall) using a semi-dry transfer system. The membrane was blocked with 5% non-fat milk for 30

min, followed by incubation with primary antibodies at specified dilutions (Parkin, 1: 1000; PINK1, 1: 1000; FUNDC1, Zenbio 251933, 1: 1000; Nrf2, 1: 1000; Keap1, Zenbio R26935, Tomm20, 1: 2000; LC3, 1: 1000; Beclin-1, CST 3738, 1: 2000; SQSTM1, Abcam ab109012, 1: 2000; β-actin, Proteintech 60008-1-lg, 1: 10000; COXIV, Zenbio 200147, 1: 3000; cGAs, HUABIO HA722736, 1: 1000; STING, HUABIO HA722832, 1: 1000; p-STING, HUABIO HA723137, 1: 1000) at room temperature for 2 h. This was followed by incubation with IRDye® 800CW fluorescent secondary antibody (1:5000; Bioss) at room temperature for 1 h, and images were obtained using an LI-COR Odyssey CLx dual-color infrared imaging system.

RNA interference

For RNA interference, siRNA targeting Nrf2 was transfected into WPMY-1 cells using the Lip RNAiMAX Transfection Reagent (HUAYUN, HYR650). A control siRNA (Negative Control siRNA) with unknown mammalian homology was used as a negative control. After 24 h of transfection, the medium was replaced, and the cells were treated with 4 μM $NaAsO_2$ for an additional 28 h. The siRNAs were designed and synthesized by Nanning Genesis Biotechnology Co., Ltd. The knockdown efficiency was tested using Western blotting. Table S2 lists siRNA sequences used for human Nrf2.

Mouse Model

Five-week-old male C57BL/6 mice were purchased from Liaoning Changsheng Biotechnology Co., Ltd. (SCXK Liao 2015-0003) and housed under specific pathogen-free (SPF) conditions at the Guangxi Medical University Experimental Animal Center. For the NAC intervention study, mice were randomly divided into five groups (n = 8/group): Ctrl (normal saline [NS]), 0.5 mg/kg $NaAsO_2$, 5 mg/kg $NaAsO_2$, 100 mg/kg NAC, and 5 mg/kg $NaAsO_2$ + NAC combined group. All treatments were administered via daily oral gavage for 90 days.

To investigate the role of mitochondrial oxidative stress, mice were randomly divided into four groups (n = 8/group): Ctrl (oral gavage of NS + intraperitoneal [i.p.] injection of NS), As (oral gavage of 5 mg/kg $NaAsO_2$ + i.p. injection of NS), Mito-TEMPO (oral gavage of NS + i.p. injection of Mito-TEMPO), and As + Mito-TEMPO (oral gavage of 5 mg/kg $NaAsO_2$ + i.p. injection of Mito-TEMPO). Mito-TEMPO was administered at 1 mg/kg via i.p. injection every other day, while $NaAsO_2$ was given daily by oral gavage.

At the end of the experimental period, prostate tissues were collected for subsequent analyses. This study was approved by the Ethics Committee of Guangxi Medical University Cancer Hospital (approval no. LW2026031).

Statistical Analysis

Statistical analysis was performed using the SPSS 22.0 (IBM, NY, USA). Body weight measurements were analyzed using repeated-measures analysis of variance (ANOVA). Other data were analyzed using one-way ANOVA, the non-parametric Kruskal-Wallis test, or t-test. Results are expressed as mean ± standard deviation (SD) or mean ± standard error (SE), with $P < 0.05$ indicating statistical significance.

Results

Arsenic induced mitochondrial damage and triggered mitophagy in WPMY-1 cells

We first studied the effects of arsenic exposure on mitochondrial homeostasis in prostate stromal cells, including mitochondrial oxidative stress, MMP and the release of mitochondrial DNA (mtDNA). The results revealed that arsenic exposure significantly induced a concentration-dependent elevation in mtROS and cellular ROS levels, with 4 μM arsenic producing the most pronounced effect (Fig. 1A-D). Pretreatment with the mitochondria-targeted antioxidant Mito-TEMPO or the general ROS scavenger NAC effectively attenuated arsenic-induced mitochondrial superoxide accumulation, confirming the critical role of mtROS in this process (Fig. 1A-D). Arsenic exposure also caused a marked decrease in MMP, which was partially restored by NAC (Fig. 1E-F). However, mtDNA release was unaffected, as downstream cGAS-STING pathway proteins remained unchanged in arsenite-treated cells (Figure S1A-B). These results indicate that mitochondrial oxidative stress drives arsenic-mediated mitochondrial injury.

To confirm whether mitophagy is involved in arsenic-induced damage, we examined mitochondrial ultrastructure and autophagic markers. Arsenite-treated cells exhibited swollen mitochondria with disrupted cristae and autophagic vacuoles encapsulating the damaged mitochondria (Fig. 1G, red arrows). Increased LC3 (autophagosome marker) and Tomm20 (mitochondrial marker) colocalization confirmed enhanced mitophagosome formation in arsenite-treated cells (Fig. 1H). Moreover, CQ, a lysosomal autophagy inhibitor, partially restored the arsenic-induced decrease in cell viability and inhibited the arsenic-induced increase in SQSTM1 and LC3 protein degradation (Fig. 1I-J, Figure S1 C). Collectively, these results demonstrate that arsenic exposure induces mitochondrial oxidative stress and dysfunction, which activates a mitophagy pathway.

Arsenic activated PINK1/Parkin mitophagy pathway

The molecular mechanism underlying arsenic-induced mitophagy was further investigated by examining the key regulators of the PINK1/Parkin pathway. Arsenic treatment significantly upregulated PINK1 and Parkin mRNA levels in a dose-dependent manner (Fig. 2A). The protein expression levels of PINK1, Parkin, Beclin-1, SQSTM1, and LC3II/I ratio were also increased (Fig. 2B, Figure S2A, 2D). Notably, FUNDC1, an alternative mitophagy receptor, remained unchanged, indicating that arsenic-induced mitophagy specifically operates through the PINK1-Parkin pathway rather than the FUNDC1-dependent pathway. Subcellular fractionation revealed that arsenic treatment promoted the translocation of LC3, Parkin and PINK1 in mitochondria (Fig. 2C, Figure S2B-C), with enhanced mitochondrial recruitment of Parkin (Fig. 2D) and increased mitochondrial retention of PINK1 (Fig. 2E) in arsenic-treated cells. We next confirmed that arsenic exposure contributes to PINK1/Parkin activation. The PINK1/Parkin pathway inhibitor CsA significantly attenuated arsenic-induced mitochondrial depolarization (Fig. 2F-G) and

partially reversed the upregulation of PINK1, Parkin, and LC3II/I ratio (Fig. 2H-I). These data collectively establish that arsenic triggers canonical PINK1/Parkin-mediated mitophagy in WPMY-1 cells.

(A) Quantitative RT-PCR analysis of PINK1, Parkin, SQSTM1, and LC3II mRNA expression levels in cells treated with 0, 1, 2, and 4 μM arsenite (As) for 48 h. Data are presented as mean ± SE. *$P < 0.05$, **$P < 0.01$. (B) Western blotting of FUNDC1, PINK1, Parkin, Beclin-1, SQSTM1, and LC3II/I in cells treated with increasing concentrations of arsenite. β-Actin served as the loading control. (C) Western blotting of Parkin, PINK1, LC3II/I, and COXIV in cytoplasmic and mitochondrial fractions of arsenite-treated cells. (D-E) Representative immunofluorescence images depicting the subcellular localization of Parkin (D) and PINK1 (E) in cells treated with or without arsenite. DAPI (blue) indicates nuclei. Scale bar = 10 μm. (F) Representative JC-1 staining images revealing MMP in cells treated with arsenite in the presence or absence of CsA, an mPTP inhibitor. (G) Quantification of MMP (red/green ratio) from panel F. **$P < 0.01$. (H) Western blotting of PINK1, Parkin, and LC3II/I in cells treated with arsenite with or without CsA. (I) Quantitative analysis of protein expression from panel H. *$P < 0.05$.

Antioxidant intervention attenuated arsenic-induced PINK1/Parkin-mediated mitophagy

Given that arsenic exposure concurrently triggers ROS and mtROS accumulation, alongside the induction of PINK1/Parkin-mediated mitophagy, we assessed whether antioxidant intervention could suppress the PINK1/Parkin pathway. Treatment with NAC significantly attenuated arsenite-induced upregulation of Parkin, PINK1, LC3II/I, and SQSTM1 (Fig. 3A, B). These effects were further validated by decreased LC3 colocalization with Tomm20 and PINK1 with Parkin (Fig. 3C, D), indicating that NAC reduced PINK1/Parkin-mediated mitophagy. To specifically target mitochondrial oxidative stress, we used Mito-TEMPO, a mitochondria-targeted antioxidant. Similar to NAC, Mito-TEMPO pretreatment effectively reversed the arsenite-induced increases in Parkin, PINK1, LC3II/I, and SQSTM1 protein levels (Fig. 3E, 3F). These findings demonstrate that pharmacological ROS scavenging effectively suppresses arsenic-induced mitophagic activation.

Arsenic-induced mitochondrial oxidative stress activated Nrf2 to promote mitophagy

Given the marked mitochondrial oxidative stress generation observed in our study (Fig. 1), and the reciprocal regulation of ROS and mtROS by Nrf2 (Bjorkman and Pereira, 2021; Cantoni et al., 2022; Jiang et al. 2024), we investigated whether arsenite-induced mitochondrial damage activates Nrf2. As expected, arsenite induced a concentration-dependent increase in Nrf2 protein expression, whereas Keap1 levels remained unchanged (Fig. 4A-B). Moreover, arsenite exposure promoted marked Nrf2 nuclear translocation, with elevated nuclear levels and increased cytoplasmic accumulation (Fig. 4C-E). Pretreatment with NAC or Mito-TEMPO significantly attenuated arsenic-induced Nrf2 upregulation (Fig. 4F, H, Figure S3) and blocked nuclear accumulation (Fig. 4G). These results established that ROS and mtROS are upstream signals for Nrf2 activation in arsenite-exposed WPMY-1 cells.

(A) Western blotting of Keap1 and Nrf2 in whole-cell lysates from cells treated with 0, 1, 2, and 4 μM arsenite. β-Actin served as the loading control. (B) Quantitative analysis of Keap1 and Nrf2 protein expression from panel A. *P < 0.05, **P < 0.01 versus the indicated group. (C) Western blotting of Nrf2 in cytoplasmic and nuclear fractions. Histone H3 served as the nuclear loading control. (D) Quantitative analysis of Nrf2 protein levels in the cytoplasmic and nuclear fractions. *P < 0.05 versus control. (E) Representative immunofluorescence images depicting Nrf2 (green) subcellular localization with DAPI (blue) nuclear staining in control and arsenite-treated cells. Scale bar = 20 um. (F) Western blotting of Nrf2 in cells treated with arsenite in the presence or absence of NAC. (G) Representative immunofluorescence images revealing Nrf2 subcellular localization in cells treated with arsenic and/or NAC. Scale bar = 10 um. (H) Western blotting of Nrf2 in cells treated with arsenic in the presence or absence of Mito-TEMPO. β-Actin served as the loading control.

Nrf2 was required for arsenic-induced PINK1/Parkin-mediated mitophagy.

Emerging evidence indicates that Nrf2 regulates mitochondrial quality control through modulating PINK1/Parkin-mediated mitophagy in hepatic and brain injury (Song et al. 2023; Li et al. 2026). Consistently, we identified that Nrf2 knockdown significantly attenuated arsenite-induced upregulation of PINK1, Parkin, and LC3II/I ratio (Fig. 5A-B, Figure S4), indicating that Nrf2 is necessary regulating of PINK1/Parkin mitophagy components in WPMY-1 cells. Besides, ML385 pretreatment markedly suppressed arsenite-induced increases in Nrf2, Parkin, PINK1, and LC3II/I ratio (Fig. 5C-D). Moreover, ML385 pretreatment reduced arsenic-induced LC3 colocalization with Tomm20 and PINK1 and Parkin (Fig. 5E-F). Collectively, these results demonstrate that Nrf2 is required for arsenic-induced PINK1/Parkin-mediated mitophagy in the prostate.

(A-B) Western blotting (A) and quantitative analysis (B) of Nrf2, Parkin, PINK1, LC3I, and LC3 in cells transfected with non-targeting control siRNA (siNTC) or Nrf2-specific siRNA (siNrf2), followed by treatment with or without arsenite (4 μM). *P < 0.05, **P < 0.01. (C-D) Western blotting (C) and quantitative analysis (D) of Nrf2, Parkin, PINK1, and LC3II/I in cells treated with arsenite in the presence or absence of ML385 (10 μM), a specific Nrf2 inhibitor. *P < 0.05, **P < 0.01. (E-F) Representative immunofluorescence images exhibiting colocalization of LC3 (green) with Tomm20 (red) and DAPI (blue) (E), and PINK1 (green) with Parkin (red) and DAPI (blue) (F) in cells treated with arsenite and ML385. Scale bar = 10 μm.

Arsenic drove mitochondrial dysfunction activated Nrf2 and PINK/Parkin-dependent mitophagy in vivo.

To confirm the physiological relevance of our *in vitro* findings, we established a mouse model of chronic arsenic exposure. Prostate weight in the arsenic-treated mice was 1.46 times that in the control group (Figure S5A). Histopathological analysis revealed disrupted glandular architecture and increased interstitial spaces in arsenic-exposed prostates, suggestive of prostatic hyperplasia (Fig. 6A). A dose-dependent upregulation of PINK1, Parkin, and SQSTM1 mRNA was observed (Fig. 6B). This trend was further validated by the elevated protein expression of PINK1, Parkin, SQSTM1, and LC3II/I (Fig. 6C-D).

Furthermore, arsenic-treated mice exhibited upregulated protein levels of Tomm20 (a key mitochondrial outer membrane translocase) and Nrf2 in the prostate (Fig. 6E-F).

For *in vivo* antioxidant intervention, NAC co-administration with arsenic ameliorated arsenic-induced histopathological alterations and significantly attenuated arsenic-induced upregulation of mitophagy markers in prostate tissues (Fig. 6A, C-D). Mito-TEMPO also effectively reversed arsenite-induced increases in LC3II/I, PINK1, Parkin, Tomm20, and Nrf2 (Fig. 6E-F). These *in vivo* data validate that arsenic exposure activates the Nrf2-mediated PINK1/Parkin mitophagy pathway in a redox-dependent manner.

(A) Hematoxylin and eosin staining of prostate tissue sections revealed histopathological changes. Scale bar = 50 μm. (B) qRT-PCR analysis of PINK1, Parkin, SQSTM1, and LC3II mRNA expression levels in prostate tissues. Data were normalized to GAPDH and presented as mean ± SE (n = 3). *P < 0.05, **P < 0.01 versus the indicated group. (C-D) Western blotting (C) and quantitative analysis (D) of SQSTM1, Parkin, PINK1, and LC3II/I in prostate tissues from mice treated with arsenite (5 mg/kg) with or without NAC (200 mg/kg). *P < 0.05, **P < 0.01 versus the indicated group. (E-F) Western blotting (E) and quantitative analysis (F) of LC3II/I, PINK1, Parkin, Nrf2, Tomm20, and COX IV in prostate tissues from mice treated with arsenic (5 mg/kg) with or without Mito-TEMPO (5 mg/kg, i.p.). *P < 0.05, **P < 0.01 versus the indicated group.

Discussion

Chronic exposure to arsenic, a pervasive environmental contaminant, represents a significant public health concern because of its association with a spectrum of diseases (McKeon et al. 2025; Qu et al. 2026; Wu et al. 2025). The prostate gland is a potential target for arsenic toxicity (Coimbra et al. 2024; Xie et al. 2020; Yang et al. 2025); however, the specific molecular pathways associating arsenic exposure to prostatic pathology remain inadequately elucidated. Although it is established that arsenic induces oxidative stress and cellular damage in the prostate(Coimbra et al. 2024; Yang et al. 2024c; Yang et al. 2025), whether Nrf2 activation and PINK1/Parkin-mediated mitophagy contribute to prostatic pathological outcomes and their reciprocal regulatory crosstalk remains to be further explored. In this study, we revealed a non-canonical signaling axis wherein arsenite exposure triggers mtROS accumulation, driving Nrf2 nuclear translocation to initiate PINK1/Parkin-mediated mitophagy in prostate cells and tissues (Fig. 7). Our study elucidates the crosstalk mechanisms among mitochondrial oxidative stress, Nrf2 signaling, and mitophagy, highlighting their potential as therapeutic targets in arsenic-induced prostate damage.

Mitochondria are dual targets of arsenic toxicity. They are both the initial sites of damage and the effectors of cell death (Ahangarpour et al. 2017; Li et al. 2022). Our prior work confirmed that arsenic-induced mitochondrial damage is a critical initiating event that triggers PANoptosis in prostate cells (Yang et al. 2025), raising the intriguing question of whether cells attempt to “self-rescue” through mitochondrial quality control mechanisms before committing to death. We observed that arsenic exposure triggered mitophagy in prostate tissue, characterized by electron microscopy and LC3

colocalization with damaged mitochondria. These observations establish that arsenic-induced mitochondrial damage initiates an active quality control response rather than passively preceding cell death. Furthermore, we observed that CQ treatment significantly rescued arsenic-induced cytotoxicity, indicating that arsenic triggered “mitophagic cell death” (Kim and Choi, 2008; Yang et al. 2024a). Mitophagic cell death can be activated by the PINK1/Parkin pathway or mitophagy receptors, including BNIP3/NIX and FUNDC1 (Chen et al. 2021; Lampert et al. 2019). PINK1/PRKN-mediated mitophagy has emerged as a dominant research focus, with extensive evidence supporting its critical role in clearing dysfunctional and depolarized mitochondria (Narendra et al. 2008; Narendra et al. 2010; Picca et al. 2023). Similarly, we also identified PINK1/Parkin-dependent mitophagy, rather than FUNDC1, as a pathological mitophagic cell death program in arsenic-treated prostatic stromal cells.

Beyond the PINK1/Parkin pathway, Nrf2 activation is also critical for preserving mitochondrial homeostasis. As a master regulator of cellular antioxidant defense, Nrf2 is vital for mediating arsenic-induced cellular injury (Qu et al. 2025; Wang et al. 2025; Xie et al. 2020; Yang et al. 2024b). However, its expression under arsenic exposure remains debated. Studies have revealed that Nrf2 exhibits a suppressive role in arsenic-regulated neuroinflammation and ferroptosis (Qu et al. 2025; Yang et al. 2024b). Conversely, in arsenic-induced oxidative stress and carcinogenesis, Nrf2 activation serves as a central regulatory node that can drive antioxidant gene and oncogene expression and promote progenitor self-renewal and epigenetic reprogramming (Kobayashi et al. 2006; Wang et al. 2025; Xie et al. 2020). In this study, we observed that arsenic exposure induces Nrf2 activation. These variations indicate that Nrf2 may play context-dependent roles in arsenic toxicity, with its function varying depending on cell or tissue type, animals, stage of toxicity, or microenvironment. Although arsenic-induced Nrf2 activation was confirmed, the specific upstream pathways governing this process remain poorly understood. Our study reveals that arsenic-induced mitochondrial damage initiates a cascade of ROS/mtROS accumulation, subsequently driving Nrf2 nuclear translocation and activating PINK1/parkin-mediated mitophagy. Notably, co-treatment with NAC and Mito-TEMPO abolished these arsenic-triggered processes, confirming mtROS as the central mediator of this cascade. This finding aligns with prior evidence associating mtROS dysregulation with arsenic-induced acute lung injury and hepatic insulin resistance (Jia et al. 2020; Li et al. 2022), suggesting a conserved mechanism across different tissue types.

Although mtROS simultaneously activates Nrf2 and PINK1/Parkin pathway, their regulatory roles under arsenic exposure remain to be confirmed. Notably, Nrf2 is a master regulator of mitophagy (Song et al. 2023; Xiao et al. 2017; Zhao et al. 2025). Studies reveal that Nrf2 can transcriptionally regulate the PINK1 genes to trigger PINK1/Parkin-mediated mitophagy (Li et al. 2026; Murata et al. 2015; Xiao et al. 2017). Similarly, in this study, Nrf2 knockdown and ML385 treatment abolished arsenite-induced PINK1/Parkin and LC3 upregulation and LC3-mitochondria colocalization in prostate stromal cells. These results confirmed that Nrf2 nuclear translocation is correlated with and mechanistically required for mitophagy initiation. However, direct evidence for Nrf2 binding to the promoter regions of PINK1, Parkin or LC3 genes remains to be further investigated. Moreover, Nrf2 establishes a critical association between

oxidative stress responses and mitophagy in arsenic toxicology, emphasizing that Nrf2 and PINK1 may provide a synergistic therapeutic strategy to restore arsenic-induced mitochondrial damage.

This study motivates several directions for future research. Elucidating the direct transcriptional targets of Nrf2 in mitophagy regulation, particularly its occupancy on PINK1 and Parkin promoters, represents an important next step. Furthermore, validating the mtROS-Nrf2-PINK1/Parkin cascade in human cohorts will bridge the gap between mechanistic insights and therapeutic translation.

In summary, this study establishes that arsenic-induced mitochondrial oxidative stress activates Nrf2, which drives PINK1/Parkin-dependent mitophagy in the prostate. This pathway was mechanistically dissected *in vitro* and was functionally associated with prostatic pathology in an arsenic-exposed mouse model. Our findings redefine the functional role of Nrf2, establishing a critical link between antioxidant signaling and mitophagy in arsenic-exposed tissues. Targeting this novel regulatory circuit may provide a promising therapeutic paradigm for arsenic-associated prostatic pathologies.

Declarations

Ethics approval

This study was approved by the Ethics Committee of Guangxi Medical University Caner Hospital (approval no. LW2026031).

Competing interest

The authors declare that they have no competing interests to disclose.

Funding

This work was financially supported by the National Natural Science Foundation of China (Grant Numbers: 82560632, 82560571), the Guangxi Yong and Middle-aged University Teachers' Scientific Research Ability Enhancement Project (Grant Number: 2025KY0135), and Young leading talents training program of Guangxi Medical University. The authors express their gratitude to the Experimental Animal Center at Guangxi Medical University for technical assistance with animal husbandry and experimental procedures.

Author Contribution

Y.P.Y., Y.H., and Y.C.J. are contributed equally to this study. Y.P.Y. and S.W. conceived and designed the study; Y.H., Y.C.J., Y.P.Y., and C.L.Z. conducted the experiments and acquired data; W.Q.L, G.L.Y. and Y.X.M. contributed to data analysis; Y.X.M. drafted the original manuscript; Q.Y.Z, Y.P.Y. and S.W. critically

revised the manuscript; Y.P.Y. and S.W. supervised the project and acquired funding. All authors have read and approved the final version of the manuscript.

Acknowledgement

The authors express their gratitude to the Experimental Animal Center at Guangxi Medical University for technical assistance with animal husbandry and experimental procedures. And we would like to give our sincere gratitude to the reviewers for their constructive comments.

Data Availability

Data will be made available on request.

References

1. Ahangarpour, A., Oroojan, A. A., Rezae, M., Khodayar, M. J., Alboghobeish, S., & Zeinvand, M. (2017). Effects of butyric acid and arsenic on isolated pancreatic islets and liver mitochondria of male mouse. Gastroenterology and hepatology from bed to bench, 10(1), 44–53.
2. Cantoni, O., Zito, E., Guidarelli, A., Fiorani, M., & Ghezzi, P. (2022). Mitochondrial ROS, ER Stress, and Nrf2 Crosstalk in the Regulation of Mitochondrial Apoptosis Induced by Arsenite. Antioxidants (Basel, Switzerland), 11(5), 1034. https://doi.org/10.3390/antiox11051034
3. Chen, J., Zhou, C., Yi, J., Sun, J., Xie, B., Zhang, Z., Wang, Q., Chen, G., Jin, S., Hou, J., Qin, M., Wang, L., & Wei, H. (2021). Metformin and arsenic trioxide synergize to trigger Parkin/pink1-dependent mitophagic cell death in human cervical cancer HeLa cells. Journal of Cancer, 12(21), 6310–6319. https://doi.org/10.7150/jca.61299
4. Coimbra, J. L. P., Campolina-Silva, G., et al. (2024). Subchronic intake of arsenic at environmentally relevant concentrations causes histological lesions and oxidative stress in the prostate of adult Wistar rats. Reproductive toxicology (Elmsford, N.Y.), 128, 108647. https://doi.org/10.1016/j.reprotox.2024.108647
5. El-Ghiaty, M. A., & El-Kadi, A. O. S. (2023). The Duality of Arsenic Metabolism: Impact on Human Health. Annual review of pharmacology and toxicology, 63, 341–358. https://doi.org/10.1146/annurev-pharmtox-051921-020936
6. Hartwick Bjorkman, S., & Oliveira Pereira, R. (2021). The Interplay Between Mitochondrial Reactive Oxygen Species, Endoplasmic Reticulum Stress, and Nrf2 Signaling in Cardiometabolic Health. Antioxidants & redox signaling, 35(4), 252–269. https://doi.org/10.1089/ars.2020.8220
7. Jia, X., Qiu, T., Yao, X., Jiang, L., Wang, N., Wei, S., Tao, Y., Pei, P., Wang, Z., Zhang, J., Zhu, Y., Yang, G., Liu, X., Liu, S., & Sun, X. (2020). Arsenic induces hepatic insulin resistance via mtROS-NLRP3 inflammasome pathway. Journal of hazardous materials, 399, 123034. https://doi.org/10.1016/j.jhazmat.2020.123034

8. Jiang, X. S., Liu, T., Xia, Y. F., Gan, H., Ren, W., & Du, X. G. (2024). Activation of the Nrf2/ARE signaling pathway ameliorates hyperlipidemia-induced renal tubular epithelial cell injury by inhibiting mtROS-mediated NLRP3 inflammasome activation. Frontiers in immunology, 15, 1342350. https://doi.org/10.3389/fimmu.2024.1342350
9. Kim, E. H., & Choi, K. S. (2008). A critical role of superoxide anion in selenite-induced mitophagic cell death. Autophagy, 4(1), 76–78. https://doi.org/10.4161/auto.5119
10. Kobayashi, A., Kang, M. I., Okawa, H., Ohtsuji, M., Zenke, Y., Chiba, T., Igarashi, K., & Yamamoto, M. (2004). Oxidative stress sensor Keap1 functions as an adaptor for Cul3-based E3 ligase to regulate proteasomal degradation of Nrf2. Molecular and cellular biology, 24(16), 7130–7139. https://doi.org/10.1128/MCB.24.16.7130-7139.2004
11. Kobayashi, A., Kang, M. I., Watai, Y., Tong, K. I., Shibata, T., Uchida, K., & Yamamoto, M. (2006). Oxidative and electrophilic stresses activate Nrf2 through inhibition of ubiquitination activity of Keap1. Molecular and cellular biology, 26(1), 221–229. https://doi.org/10.1128/MCB.26.1.221-229.2006
12. Lampert, M. A., Orogo, A. M., Najor, R. H., Hammerling, B. C., Leon, L. J., Wang, B. J., Kim, T., Sussman, M. A., & Gustafsson, Å. B. (2019). BNIP3L/NIX and FUNDC1-mediated mitophagy is required for mitochondrial network remodeling during cardiac progenitor cell differentiation. Autophagy, 15(7), 1182–1198. https://doi.org/10.1080/15548627.2019.1580095
13. Li, M. D., Fu, L., Lv, B. B., Xiang, Y., Xiang, H. X., Xu, D. X., & Zhao, H. (2022). Arsenic induces ferroptosis and acute lung injury through mtROS-mediated mitochondria-associated endoplasmic reticulum membrane dysfunction. Ecotoxicology and environmental safety, 238, 113595. https://doi.org/10.1016/j.ecoenv.2022.113595
14. Li, Z., Xu, W., Ren, S., Zheng, Q., & Xing, J. (2026). Curcumin augments mitophagy via Nrf2-PINK1-mediated, Parkin-dependent ubiquitination to suppress ferroptosis in post-cardiac arrest brain injury. Phytomedicine: international journal of phytotherapy and phytopharmacology, 154, 158035. https://doi.org/10.1016/j.phymed.2026.158035
15. Liu, S., Liu, Y., Li, J., Wang, M., Chen, X., Gan, F., Wen, L., Huang, K., & Liu, D. (2023). Arsenic Exposure-Induced Acute Kidney Injury by Regulating SIRT1/PINK1/Mitophagy Axis in Mice and in HK-2 Cells. Journal of agricultural and food chemistry, 71(42), 15809–15820. https://doi.org/10.1021/acs.jafc.3c05341
16. McKeon, H. P., Chen, W., et al. (2025). Urinary concentrations of arsenic species in older Dutch adults and risk of chronic kidney disease. Environment international, 196, 109289. https://doi.org/10.1016/j.envint.2025.109289
17. Murata, H., Takamatsu, H., Liu, S., Kataoka, K., Huh, N. H., & Sakaguchi, M. (2015). NRF2 Regulates PINK1 Expression under Oxidative Stress Conditions. PloS one, 10(11), e0142438. https://doi.org/10.1371/journal.pone.0142438
18. Narendra, D. P., Jin, S. M., Tanaka, A., Suen, D. F., Gautier, C. A., Shen, J., Cookson, M. R., & Youle, R. J. (2010). PINK1 is selectively stabilized on impaired mitochondria to activate Parkin. PLoS biology,

8(1), e1000298. https://doi.org/10.1371/journal.pbio.1000298

19. Narendra, D., Tanaka, A., Suen, D. F., & Youle, R. J. (2008). Parkin is recruited selectively to impaired mitochondria and promotes their autophagy. The Journal of cell biology, 183(5), 795–803. https://doi.org/10.1083/jcb.200809125
20. O'Mealey, G. B., Plafker, K. S., Berry, W. L., Janknecht, R., Chan, J. Y., & Plafker, S. M. (2017). A PGAM5-KEAP1-Nrf2 complex is required for stress-induced mitochondrial retrograde trafficking. Journal of cell science, 130(20), 3467–3480. https://doi.org/10.1242/jcs.203216
21. Peng, Z., Yang, Q., Yeerken, R., Chen, J., Liu, X., & Li, X. (2022). Multi-omics analyses reveal the mechanisms of Arsenic-induced male reproductive toxicity in mice. Journal of hazardous materials, 424(Pt C), 127548. https://doi.org/10.1016/j.jhazmat.2021.127548
22. Picca, A., Faitg, J., Auwerx, J., Ferrucci, L., & D'Amico, D. (2023). Mitophagy in human health, ageing and disease. Nature metabolism, 5(12), 2047–2061. https://doi.org/10.1038/s42255-023-00930-8
23. Qu, J., Jiang, X., Ma, Y., et al. (2026). Unveiling the gut-brain axis: How chronic exposure to arsenic-induced microglial pyroptosis drives Alzheimer's disease-like pathology. Journal of hazardous materials, 503, 141087. https://doi.org/10.1016/j.jhazmat.2026.141087
24. Qu, J., Pi, C., Ma, Y., Jiang, X., Sheng, X., Wang, Y., Yi, J., Wu, J., Wang, J., Wen, L., & Liu, S. (2025). Chronic Arsenic Exposure Induces Neuroinflammation by Regulating the Nrf2/NLRP3 Inflammasome Signaling Pathway. Journal of agricultural and food chemistry, 73(50), 31853–31864. https://doi.org/10.1021/acs.jafc.5c12523
25. Song, C., Zhang, A., Zhang, M., Song, Y., Huangfu, H., Jin, S., Sun, Y., Zhang, C., Shi, D., Wang, J., Peng, W., & Luo, Q. (2023). Nrf2/PINK1-mediated mitophagy induction alleviates sodium fluoride-induced hepatic injury by improving mitochondrial function, oxidative stress, and inflammation. Ecotoxicology and environmental safety, 252, 114646. https://doi.org/10.1016/j.ecoenv.2023.114646
26. Wang, S., Long, H., Hou, L., Feng, B., Ma, Z., Wu, Y., Zeng, Y., Cai, J., Zhang, D. W., & Zhao, G. (2023). The mitophagy pathway and its implications in human diseases. Signal transduction and targeted therapy, 8(1), 304. https://doi.org/10.1038/s41392-023-01503-7
27. Wang, Z., Bi, Z., Bamrah, J., Qiu, Y., Zhang, W., Almutairy, B. S., Ji, H., Haley, J. D., Thakur, C., & Chen, F. (2025). Nrf2 Drives Epigenetic Reprogramming and Acts as the Master Regulator of KLF4 Expression and Activity in Arsenic-Induced Transformation. Advanced science (Weinheim, Baden-Wurttemberg, Germany), 12(40), e00221. https://doi.org/10.1002/advs.202500221
28. Wei, S., Qiu, T., Yao, X., Wang, N., Jiang, L., Jia, X., Tao, Y., Wang, Z., Pei, P., Zhang, J., Zhu, Y., Yang, G., Liu, X., Liu, S., & Sun, X. (2020). Arsenic induces pancreatic dysfunction and ferroptosis via mitochondrial ROS-autophagy-lysosomal pathway. Journal of hazardous materials, 384, 121390. https://doi.org/10.1016/j.jhazmat.2019.121390
29. Wu, F., van Geen, A., Graziano, J.,et al. (2025). Arsenic Exposure Reduction and Chronic Disease Mortality. JAMA, 334(23), 2104–2112. https://doi.org/10.1001/jama.2025.19161

30. Wu, F., Wang, Y., Li, S., Xu, Z., Wang, X., Yin, H., Ma, T., & Wang, L. (2026). Arsenic Exposure Induces Hepatic Fibrosis and Triggers Early Inflammatory Responses by Inhibiting Hepatic Stellate Cell PINK1/Parkin-Mediated Mitophagy. Biological trace element research, 10.1007/s12011-026-05207-1. Advance online publication. https://doi.org/10.1007/s12011-026-05207-1
31. Xiao, L., Xu, X., Zhang, F., Wang, M., Xu, Y., Tang, D., Wang, J., Qin, Y., Liu, Y., Tang, C., He, L., Greka, A., Zhou, Z., Liu, F., Dong, Z., & Sun, L. (2017). The mitochondria-targeted antioxidant MitoQ ameliorated tubular injury mediated by mitophagy in diabetic kidney disease via Nrf2/PINK1. Redox biology, 11, 297–311. https://doi.org/10.1016/j.redox.2016.12.022
32. Xie, L., Hu, W. Y., Hu, D. P., Shi, G., Li, Y., Yang, J., & Prins, G. S. (2020). Effects of Inorganic Arsenic on Human Prostate Stem-Progenitor Cell Transformation, Autophagic Flux Blockade, and NRF2 Pathway Activation. Environmental health perspectives, 128(6), 67008. https://doi.org/10.1289/EHP6471
33. Yang, M., Wei, X., Yi, X., & Jiang, D. S. (2024a). Mitophagy-related regulated cell death: molecular mechanisms and disease implications. Cell death & disease, 15(7), 505. https://doi.org/10.1038/s41419-024-06804-5
34. Yang, X., Chu, F., Jiao, Z., Yu, H., Yang, W., Li, Y., Lu, C., Ma, H., Wang, S., Liu, Z., Qin, S., & Sun, H. (2024b). Ellagic acid ameliorates arsenic-induced neuronal ferroptosis and cognitive impairment via Nrf2/GPX4 signaling pathway. Ecotoxicology and environmental safety, 283, 116833. https://doi.org/10.1016/j.ecoenv.2024.116833
35. Yang, Y., Chen, X., Deng, L., Huang, Y., Mo, Y., Ye, J., Liang, R., Qin, Y., Zhang, Q., & Wang, S. (2025). Arsenic exposure provoked prostatic PANoptosis by inducing mitochondrial dysfunction in mice and WPMY-1 cells. Ecotoxicology and environmental safety, 295, 118139. https://doi.org/10.1016/j.ecoenv.2025.118139
36. Yang, Y., Zhou, M., Huang, Y., Ye, X., Mo, Y., Huang, Y., & Wang, S. (2024c). LCP1-mediated cytoskeleton alterations involve in arsenite-triggered malignant phenotype of human immortalized prostate stromal cells. Food and chemical toxicology: an international journal published for the British Industrial Biological Research Association, 186, 114548. https://doi.org/10.1016/j.fct.2024.114548
37. Zhang, Q., Man, J., Cai, J., Zhao, T., & Zhang, Z. (2026). YTHDF2 promotes arsenic carcinogenesis through m6A-dependent SMAD7 decay and PRR5 escape from decay. International journal of biological macromolecules, 348, 150816. https://doi.org/10.1016/j.ijbiomac.2026.150816
38. Zhang, Y., Song, J., Wan, S., Huo, Z., Liu, Q., Hong, L., Xiong, Y., Wang, F., Zhang, M., Xiong, G., Chen, P., Liang, R., Guo, Y., Wang, B., & Chen, W. (2026). Arsenic exposure, arsenic metabolism, and plasma lipidome in relation to type 2 diabetes and glycemic traits: a lipidome-wide association study. Journal of advanced research, 87, 607–620. https://doi.org/10.1016/j.jare.2025.12.009
39. Zhao, Y., Xiong, R., Jin, S., Li, Y., Dong, T., Wang, W., Song, X., & Guan, C. (2025). MitoQ alleviates H2O2-induced mitochondrial dysfunction in keratinocytes through the Nrf2/PINK1 pathway. Biochemical pharmacology, 234, 116811. https://doi.org/10.1016/j.bcp.2025.116811

Figures

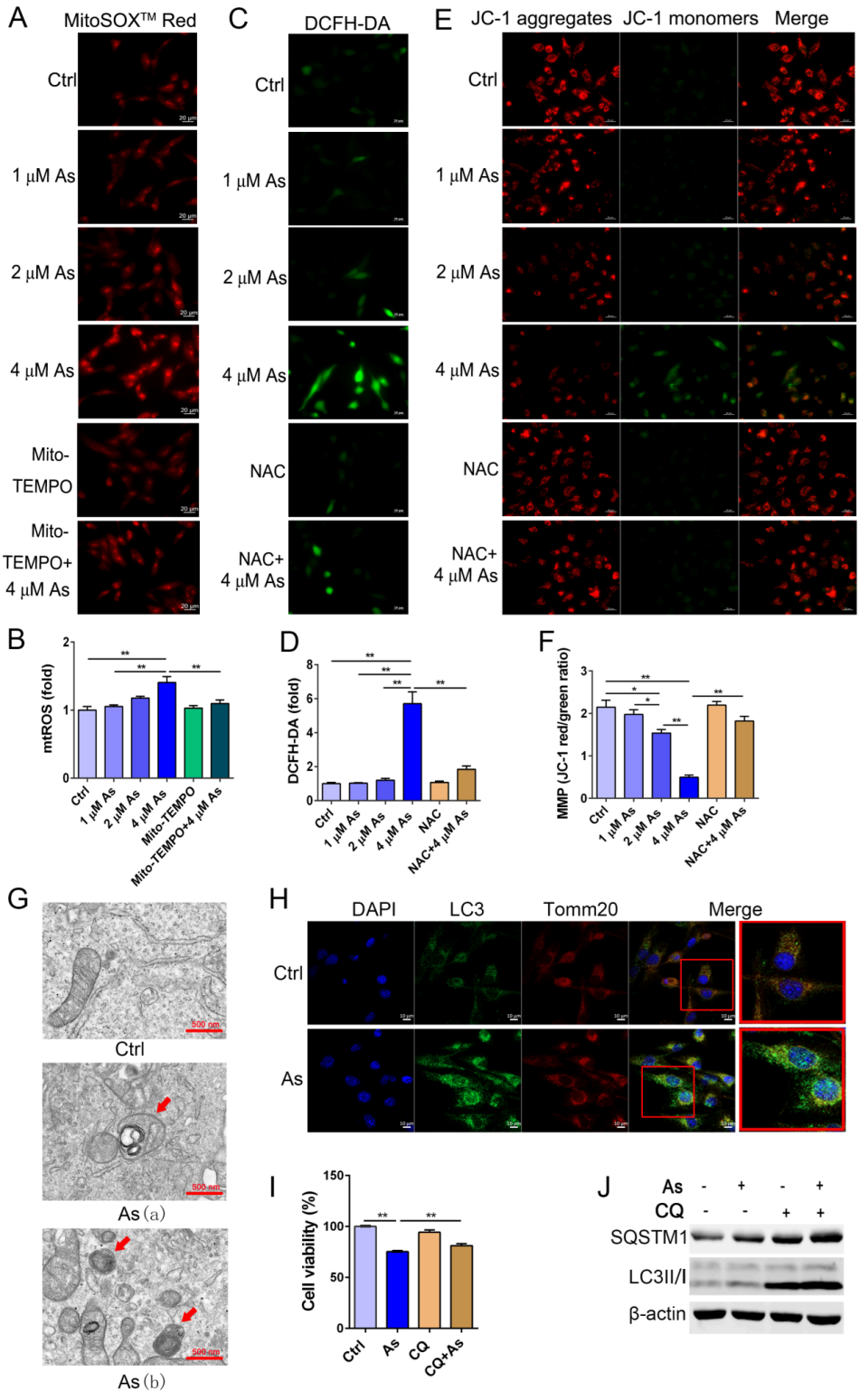

Figure 1

Arsenic induces mitochondrial damage and mitophagy in WPMY-1 cells. (A) Representative fluorescence images of MitoSOX™ Red staining exhibiting mitochondrial superoxide levels in WPMY-1 cells exposed to 0, 1, 2, and 4 μM sodium arsenite (As) for 48 h, with or without Mito-TEMPO pretreatment. Scale bar = 20

μm. (B) Quantification of mtROS levels expressed as fold change relative to control. (C) Representative fluorescence images of DCFH-DA staining indicating cellular ROS levels in cells treated with arsenite, with or without NAC pretreatment. Scale bar = 20 μm. (D) Quantitative analysis of DCFH-DA fluorescence intensity. (E) Representative fluorescence images of JC-1 staining exhibiting MMP. Red fluorescence indicates JC-1 aggregates (polarized mitochondria), whereas green fluorescence indicates JC-1 monomers (depolarized mitochondria). Scale bar = 20 μm. (F) Quantitative analysis of MMP (red/green ratio) from panel C. Data in B, D, and F are presented as mean ± SE. *$P < 0.05$, **$P < 0.01$. (G) TEM images exhibiting autophagic vacuoles containing mitochondria (indicated by red arrows) after 48 h of arsenite exposure. Scale bar = 500 nm. (H) Representative immunofluorescence images revealing colocalization of LC3 (green) with Tomm20 (red), indicating mitophagosome formation. Scale bar = 10 μm. (I) Cell viability assay exhibiting the effect of CQ on arsenic-induced cytotoxicity. Data are presented as mean ± SE (n = 4). **$P < 0.01$. (J) Western blotting of SQSTM1 and LC3II/I in cells treated with arsenite and/or chloroquine.

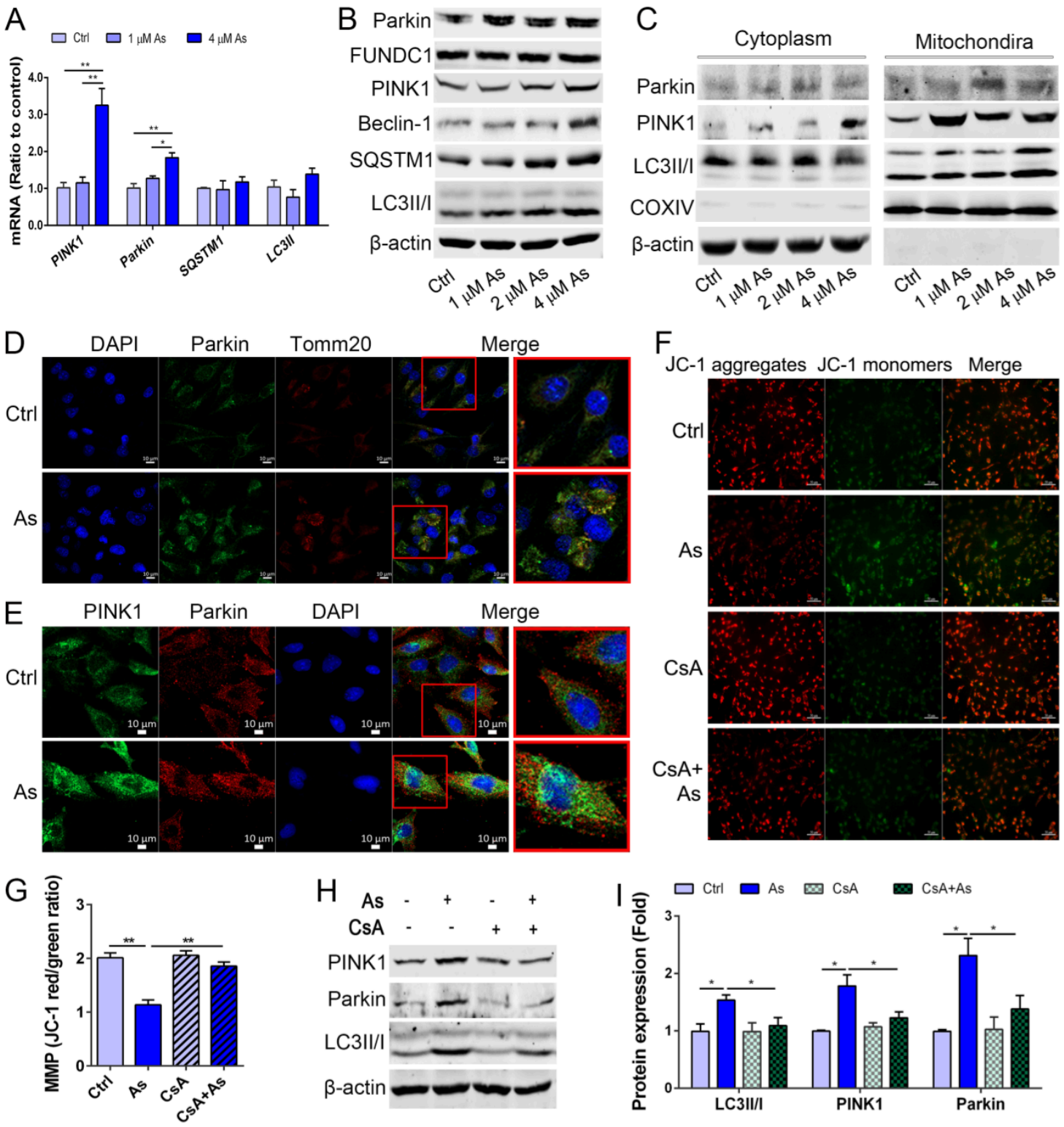

Figure 2

Arsenic activates the PINK1/Parkin-mediated mitophagy pathway in WPMY-1 cells.

(A) Quantitative RT-PCR analysis of PINK1, Parkin, SQSTM1, and LC3II mRNA expression levels in cells treated with 0, 1, 2, and 4 μM arsenite (As) for 48 h. Data are presented as mean ± SE. *$P < 0.05$, **$P < 0.01$. (B) Western blotting of FUNDC1, PINK1, Parkin, Beclin-1, SQSTM1, and LC3II/I in cells treated with

increasing concentrations of arsenite. β-Actin served as the loading control. (C) Western blotting of Parkin, PINK1, LC3II/I, and COXIV in cytoplasmic and mitochondrial fractions of arsenite-treated cells. (D-E) Representative immunofluorescence images depicting the subcellular localization of Parkin (D) and PINK1 (E) in cells treated with or without arsenite. DAPI (blue) indicates nuclei. Scale bar = 10 μm. (F) Representative JC-1 staining images revealing MMP in cells treated with arsenite in the presence or absence of CsA, an mPTP inhibitor. (G) Quantification of MMP (red/green ratio) from panel F. ***P*< 0.01. (H) Western blotting of PINK1, Parkin, and LC3II/I in cells treated with arsenite with or without CsA. (I) Quantitative analysis of protein expression from panel H. **P* < 0.05.

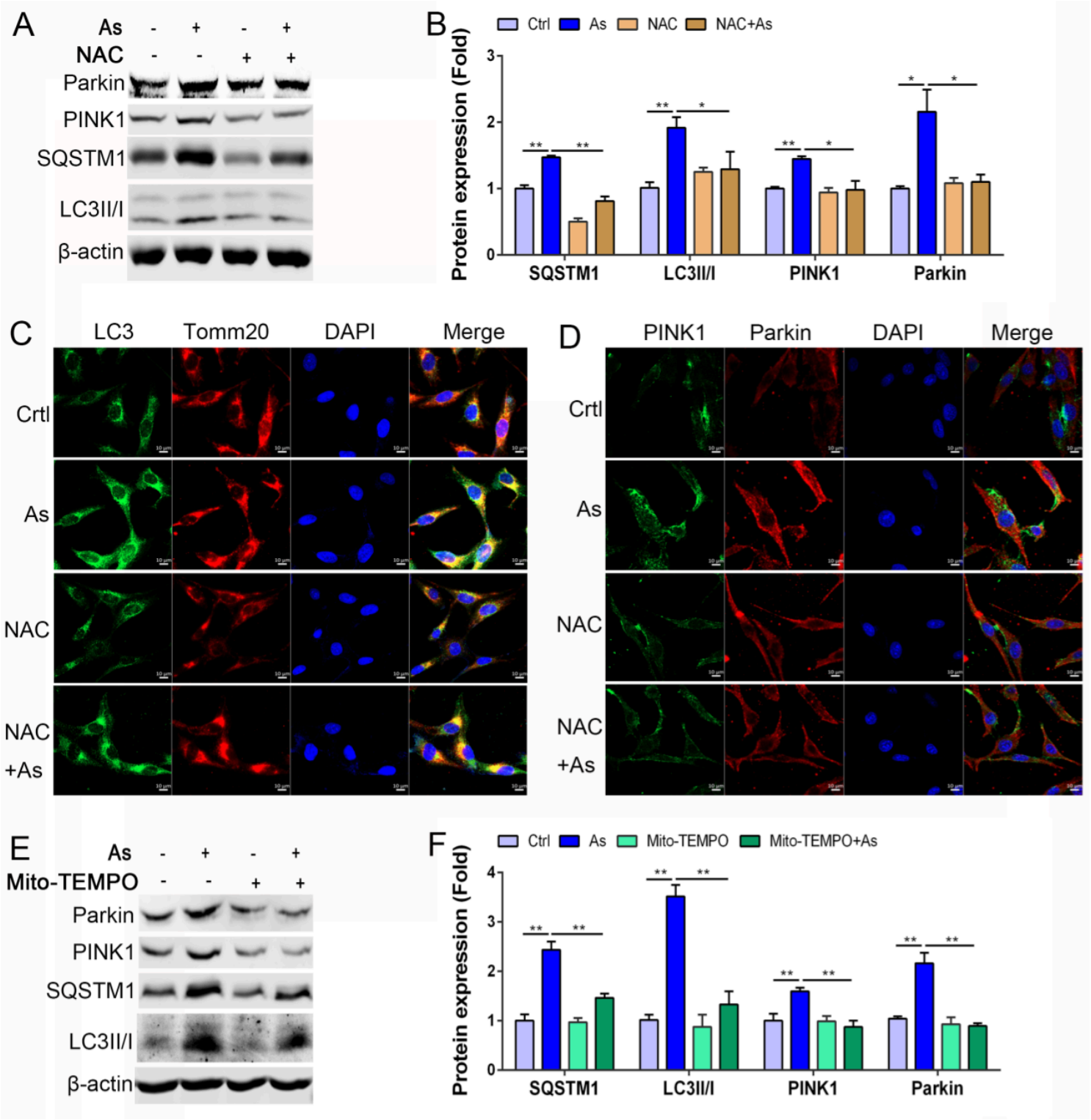

Figure 3

Antioxidant intervention attenuates arsenic-induced PINK1/Parkin-mediated mitophagy. (A-B) Western blotting (A) and quantitative analysis (B) of Parkin, PINK1, SQSTM1, and LC3II/I in cells treated with arsenic in the presence or absence of NAC. *P < 0.05, **P< 0.01. (C-D) Representative immunofluorescence images exhibiting colocalization of LC3 (green) with Tomm20 (red) (C) and PINK1 (green) with Parkin (red) in cells treated with arsenic and/or NAC. Scale bar = 10 μm. (E, F) Western

blotting (E) and quantitative analysis (F) of Parkin, PINK1, SQSTM1, and LC3II/I in cells treated with arsenic in the presence or absence of Mito-TEMPO (60 μM). **$P < 0.05$, **$P < 0.01$ versus the indicated group.

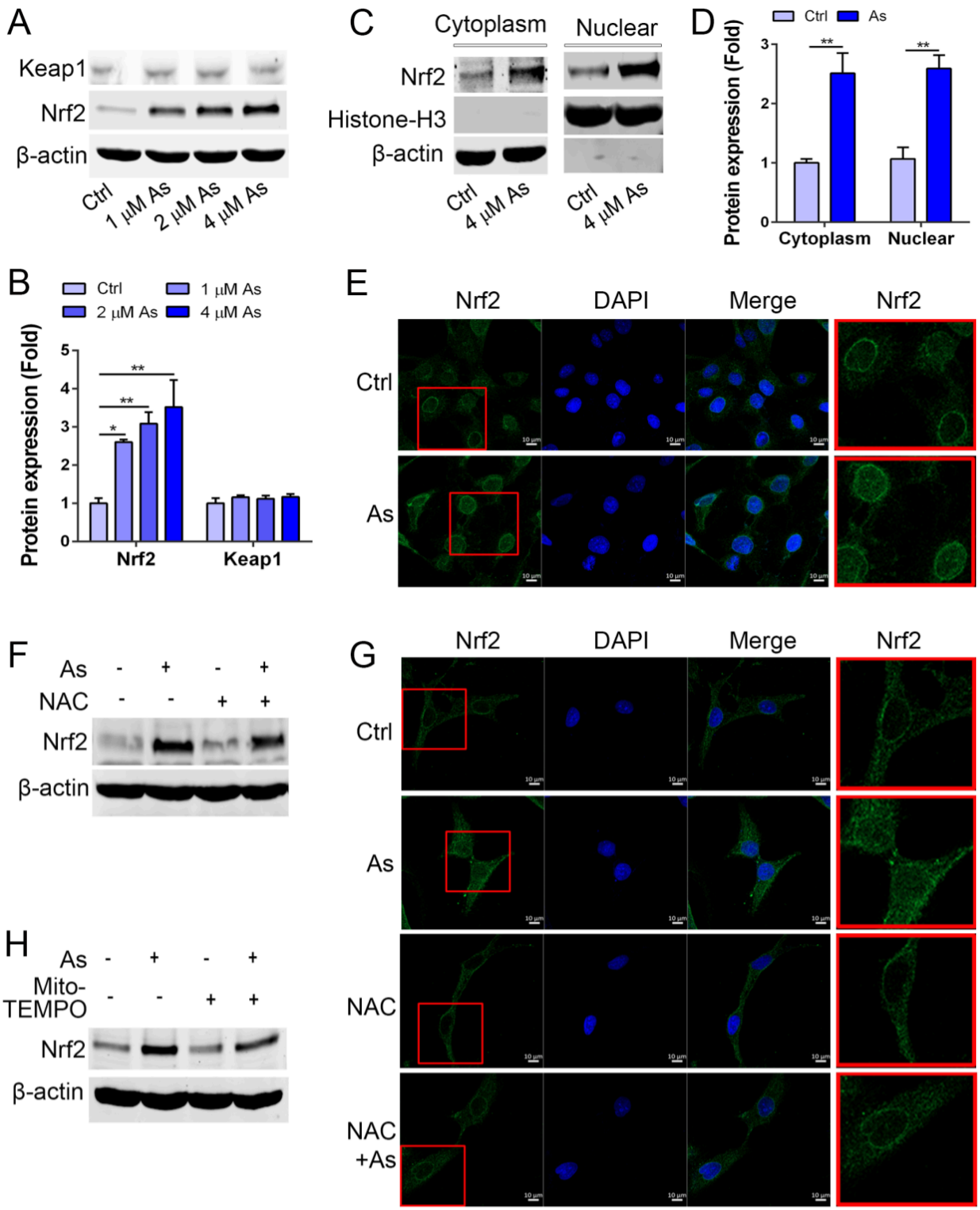

Figure 4

Arsenic-induced mitochondrial damage activates the Nrf2 signaling pathway.

(A) Western blotting of Keap1 and Nrf2 in whole-cell lysates from cells treated with 0, 1, 2, and 4 μM arsenite. β-Actin served as the loading control. (B) Quantitative analysis of Keap1 and Nrf2 protein expression from panel A. *P < 0.05, **P < 0.01 versus the indicated group. (C) Western blotting of Nrf2 in cytoplasmic and nuclear fractions. Histone H3 served as the nuclear loading control. (D) Quantitative analysis of Nrf2 protein levels in the cytoplasmic and nuclear fractions. *P < 0.05 versus control. (E) Representative immunofluorescence images depicting Nrf2 (green) subcellular localization with DAPI (blue) nuclear staining in control and arsenite-treated cells. Scale bar = 20 um. (F) Western blotting of Nrf2 in cells treated with arsenite in the presence or absence of NAC. (G) Representative immunofluorescence images revealing Nrf2 subcellular localization in cells treated with arsenic and/or NAC. Scale bar = 10 um. (H) Western blotting of Nrf2 in cells treated with arsenic in the presence or absence of Mito-TEMPO. β-Actin served as the loading control.

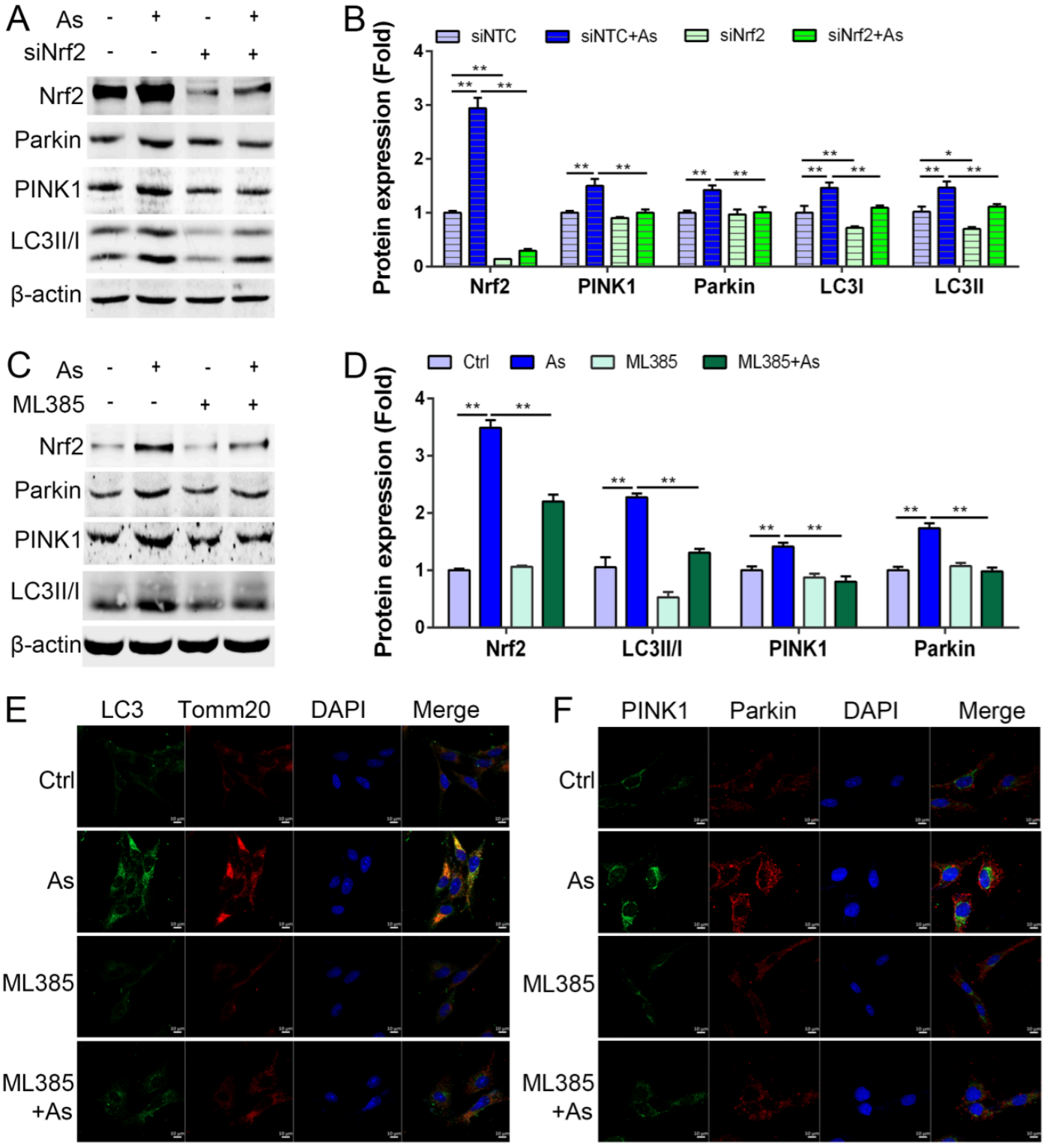

Figure 5

Nrf2 mediates arsenic-induced PINK1/Parkin-dependent mitophagy.

(A-B) Western blotting (A) and quantitative analysis (B) of Nrf2, Parkin, PINK1, LC3I, and LC3 in cells transfected with non-targeting control siRNA (siNTC) or Nrf2-specific siRNA (siNrf2), followed by treatment with or without arsenite (4 μM). *$P < 0.05$, **$P < 0.01$. (C-D) Western blotting (C) and

quantitative analysis (D) of Nrf2, Parkin, PINK1, and LC3II/I in cells treated with arsenite in the presence or absence of ML385 (10 μM), a specific Nrf2 inhibitor. *P< 0.05, **P < 0.01. (E-F) Representative immunofluorescence images exhibiting colocalization of LC3 (green) with Tomm20 (red) and DAPI (blue) (E), and PINK1 (green) with Parkin (red) and DAPI (blue) (F) in cells treated with arsenite and ML385. Scale bar = 10 μm.

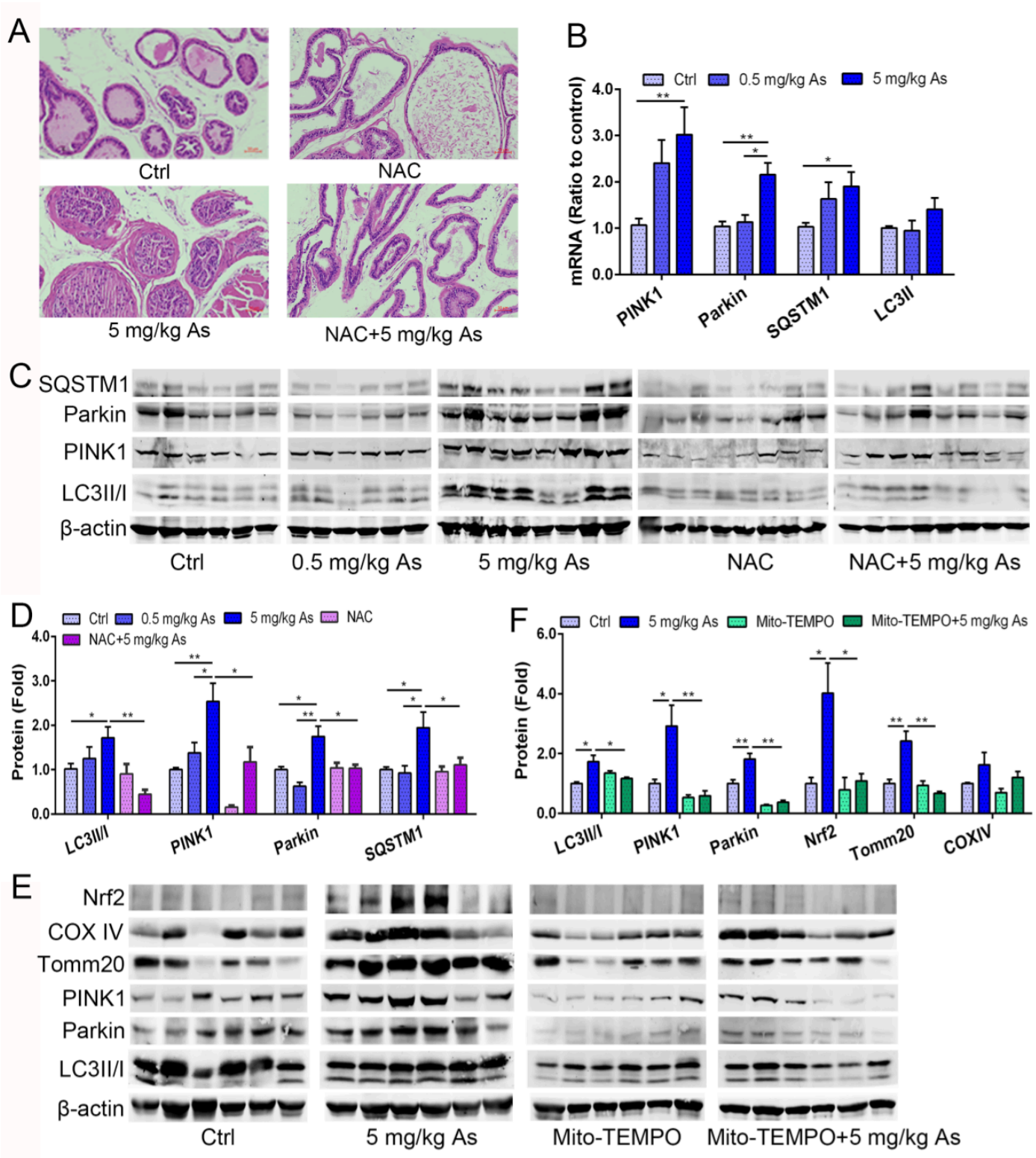

Figure 6

Validation of arsenic drives mitochondrial dysfunction activated Nrf2 and PINK/Parkin-dependent mitophagy *in vivo*.

(A) Hematoxylin and eosin staining of prostate tissue sections revealed histopathological changes. Scale bar = 50 μm. (B) qRT-PCR analysis of PINK1, Parkin, SQSTM1, and LC3II mRNA expression levels in prostate tissues. Data were normalized to GAPDH and presented as mean ± SE (n = 3). *P < 0.05, **P< 0.01 versus the indicated group. (C-D) Western blotting (C) and quantitative analysis (D) of SQSTM1, Parkin, PINK1, and LC3II/I in prostate tissues from mice treated with arsenite (5 mg/kg) with or without NAC (200 mg/kg). *P < 0.05, **P < 0.01 versus the indicated group. (E-F) Western blotting (E) and quantitative analysis (F) of LC3II/I, PINK1, Parkin, Nrf2, Tomm20, and COX IV in prostate tissues from mice treated with arsenic (5 mg/kg) with or without Mito-TEMPO (5 mg/kg, i.p.). *P < 0.05, **P< 0.01 versus the indicated group.

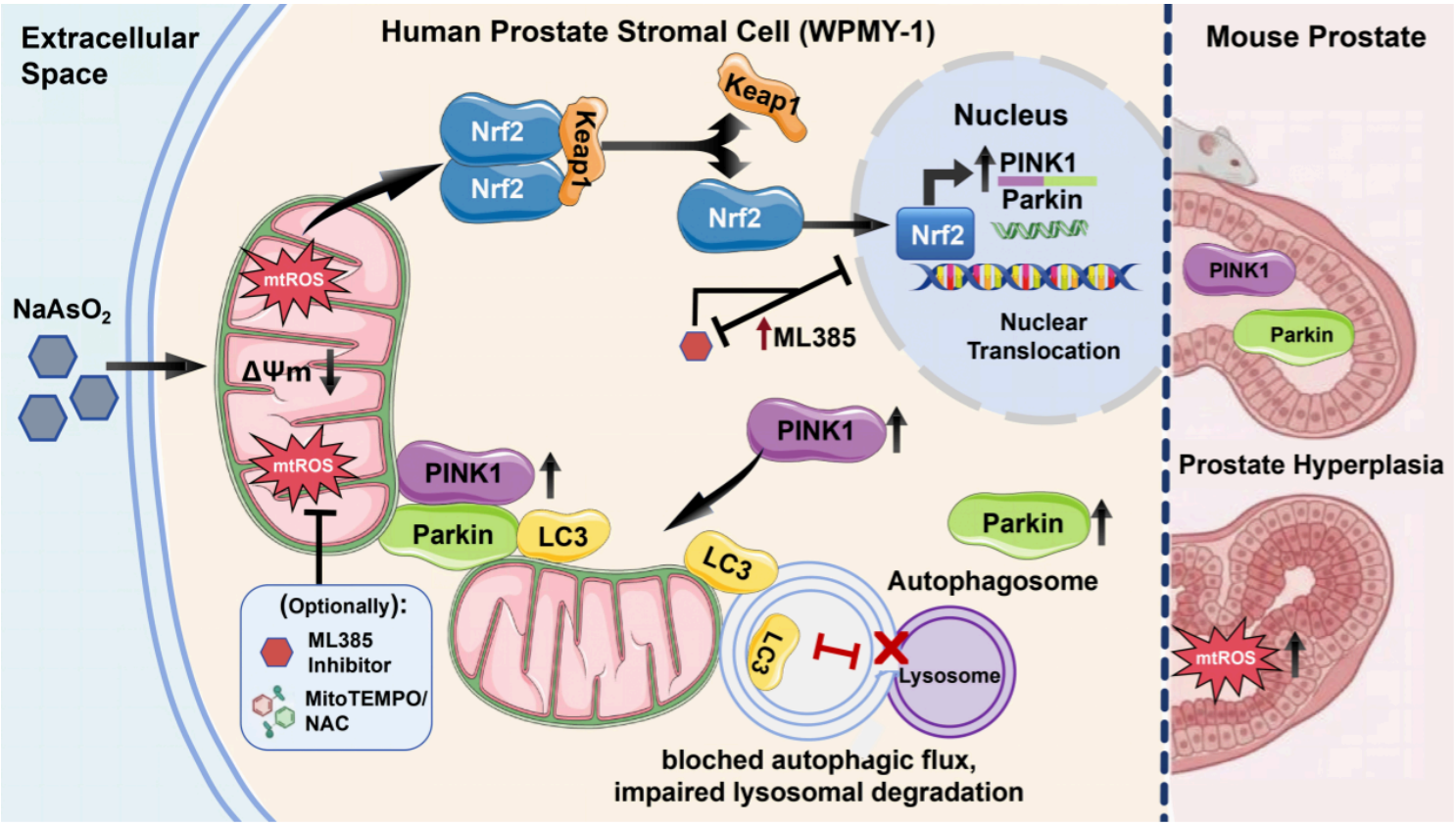

Figure 7

Schematic illustration of the mtROS-Nrf2-PINK1/Parkin axis in arsenic-induced prostatic hyperplasia. In human prostate stromal cells (WPMY-1), $NaAsO_2$ induces mitochondrial dysfunction with elevated mtROS and membrane potential loss. mtROS triggers Keap1 oxidation and Nrf2 nuclear translocation, which transcriptionally upregulates PINK1 and Parkin to initiate mitophagy. However, autophagic flux is blocked at the lysosomal degradation stage, causing the accumulation of damaged mitochondria. Pharmacological interventions (ML385, Mito-TEMPO, and NAC) reversed this process. In mice, chronic

arsenic exposure elevates prostate mtROS and then activates Nrf2 and PINK1/Parkin-mediated mitophagy, leading to prostatic hyperplasia.

Supplementary Files

This is a list of supplementary files associated with this preprint. Click to download.

- SupplementaryTable1.docx
- SupplementaryTable2.docx
- FiguresS15.pdf
- SupplementaryFigurelegends0724.docx.docx
- SupplementaryFig.1Uncroppedgelsandblots.pdf
- SupplementaryFig.2Uncroppedgelsandblots.pdf
- SupplementaryFig.3Uncroppedgelsandblots.pdf
- SupplementaryFig.4Uncroppedgelsandblots.pdf
- SupplementaryFig.5Uncroppedgelsandblots.pdf
- SupplementaryFig.6Uncroppedgelsandblots.pdf
- SupplementaryFig.S1Uncroppedgelsandblots.pdf
- SupplementaryFig.S4Uncroppedgelsandblots.pdf